Vancomycin-Modified Nanoparticles for Efficient Targeting and Preconcentration of Gram-Positive and Gram-Negative Bacteria

Arnold J. Kell,[†] Gale Stewart,[§] Shannon Ryan,[‡] Regis Peytavi,[§] Maurice Boissinot,[§] Ann Huletsky,[§] Michel G. Bergeron,[§] and Benoit Simard[†,*]

[†]Contribution from Steacie Institute for Molecular Sciences, National Research Council of Canada, 100 Sussex Drive, Ottawa, Ontario, Canada K1A 0R6, [‡]Institute for Biological Sciences, National Research Council of Canada, 100 Sussex Drive, Ottawa, Ontario, Canada K1A 0R6, and [§]Centre de Recherche en Infectiologie, Centre Hospitalier Universitaire de Québec, Pavillon CHUL, Université Laval, Québec, Québec, Canada G1V 4G2

ABSTRACT A series of vancomycin-modified nanoparticles were developed and employed in magnetic confinement assays to isolate a variety of Gram-positive and Gram-negative bacteria from aqueous solution. We determined that the orientation/architecture of vancomycin on the surface of the nanoparticles and the overall surface coverage is critical in mediating fast and effective interactions between the nanoparticle and the pathogen cell wall surface and only one orientation/architecture in a series of modified nanoparticles leads to the efficient and reproducible capture of several important pathogenic bacteria. Interestingly, as the nanoparticles increase in diameter (from ~50 to 2800 nm), it is necessary to incorporate a long linker between the nanoparticle surface and the vancomycin moiety in order for the surface bound probe to efficiently confine Gram-positive bacteria. Finally, we also determined that the time required for efficient labeling and subsequent magnetic confinement significantly decreases as the size of the nanoparticle and the vancomycin surface coverage on the nanoparticle increases. As disease detection technologies transition to "lab-on-a-chip" based platforms it is necessary to develop strategies to effectively and inexpensively preconcentrate cells from large volume to volumes more amenable to these types of microfluidic devices. These small molecule-modified superparamagnetic nanoparticles can provide a means by which this can be accomplished.

KEYWORDS: vancomycin · molecular orientation/architecture · superparamagnetic nanoparticle · magnetic concentration · bacteria

Infectious diseases are one of the world's most pressing health challenges and the development of strategies capable of quickly identifying infections presents a difficult challenge because most of the diagnostic applications currently employed are slow, expensive, and are not practical for point-of-care or field applications.[1] To expedite the identification of pathogens (viruses, bacteria, and fungi), an elegant and innovative new approach involves the development of microfluidic platforms where the pathogens can be ruptured/lysed[2] and subsequently detected and identified based on their genomic DNA.[3,4] Within such a strategy there are many opportunities where research in nanotechnology and nanomaterials can aid in the detection and identification of infectious diseases. For example, there are obvious problems associated with identifying pathogens from the large sample volumes of clinical blood samples (10−20 mL) on microfluidic system platforms, which generally handle only 50−200 μL volumes. To address this problem it is possible to utilize functionalized superparamagnetic nanoparticles (NPs) to specifically interact with pathogens and impart magnetic character to them. Following this "magnetization", it should be possible to magnetically concentrate the pathogen from large sample volumes into much smaller volumes, allowing their incorporation onto a microfluidic device platform for analysis and detection based on, for example, their genomic DNA. There are a number of other strategies that employ magnetic nanoparticles for the rapid detection of pathogens that have readouts less definitive than a DNA fingerprint. These methods include TEM,[5] MALDI-MS,[6] combined magnetic/luminescence-based assays,[7] and magnetic bead-based immunological assays.[8−10] Regardless of the detection strategy, it is imperative that the nanoparticle effectively and specifically targets a given pathogen (or more broadly, a biomolecule). This can only be accomplished by properly functionalizing its surface with substrates capable of selectively and strongly interacting with surface groups on the biomolecule of interest. Antibody-modified particles have found success in cell/biomolecule labeling experiments. However, antibodies are specific to

*Address correspondence to benoit.simard@cnrc-nrc.ca.

Received for review August 20, 2007 and accepted August 05, 2008.

Published online August 21, 2008.
10.1021/nn700183g CCC: $40.75

one species or family of pathogen[8−10] and are very large molecules with many functional groups which can limit the number of antibodies that can be anchored to the surface while allowing those that do bind to adopt orientations not suitable for antigen binding (*i.e.*, may be bound with the binding site facing the nanoparticle surface).[11] A more attractive solution is the use of small molecule probes.

Small molecule probes have emerged as important substrates capable of mediating relatively strong interactions between nanoparticles and cells/biomolecules. A number of research groups have utilized small molecule probe-modified nanoparticles to effectively label bacteria,[5,6,12,13] and cancer cells.[14−17] Small molecule probes are particularly attractive for mediating interactions between nanoparticles and cells because they generally possess only a few functional groups capable of participating in standard bioconjugation reactions. As such, one can exert orientational/architectural control over the attachment of the molecules to nanoparticle surfaces. Here we report that a small molecule probe, vancomycin, can be anchored to the surface of a series of magnetic particles in two distinct orientations through two distinct architectures. For the smallest nanoparticles (~50 nm in diameter) one of the orientations/architectures mediates more effective magnetic capture efficiencies for several bacteria species in comparison to the other. However, as the nanoparticles increase in size the consistency of the capture for the series of bacteria is lost unless the vancomycin moiety is extended from the surface with a diethylene glycol linker molecule.

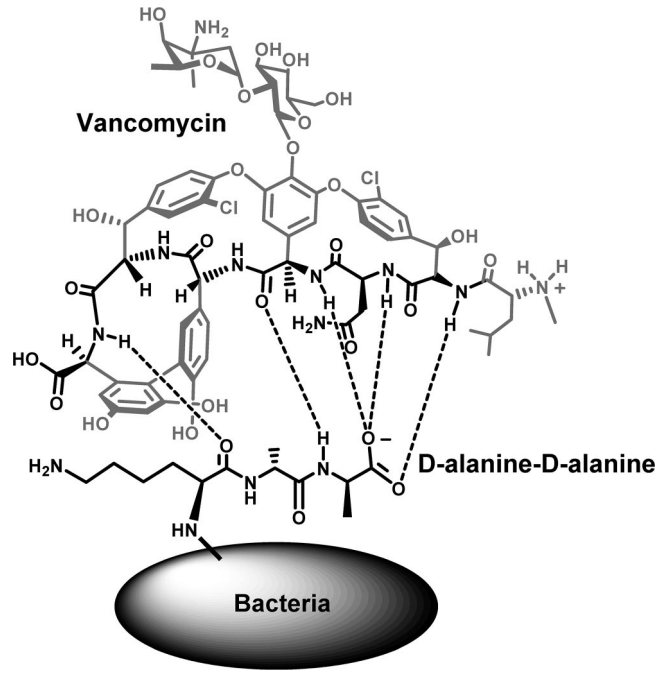

Figure 1. Cartoon representation of the vancomycin-D-alanyl-D-alanine interaction responsible for mediating the interaction between the nanoparticles and the bacteria. The critical components for the strong H-bonding interaction both on the vancomycin molecule (the heptapeptide backbone) and the D-alanyl-D-alanine dipeptide exposed from the bacterial surface are highlighted.

RESULTS AND DISCUSSION

Vancomycin is a well-known glycopeptide antibiotic capable of strongly interacting with a broad range of Gram-positive bacteria.[18,19] It interacts with bacterial cells through a surprisingly simple five-hydrogen bond motif between the heptapeptide backbone of vancomycin (darkened in Figure 1) and the D-alanyl-D-alanine dipeptide (also darkened in Figure 1) extending from the cell wall.[18,19] The interaction is quite strong with respect to small molecule−biomolecule interactions, with a dissociation constant (K_d) of ~1−4 μM at pH 7 (similar to many antibody−antigen interactions (K_d = 1 μM−1 fM).[20,21] Though vancomycin offers less specificity/selectivity than monoclonal antibodies, it is very attractive as a ligand allowing affinity capture of a wide range of bacteria with a single vancomycin-functionalized nanoparticle. This is ideal in situations where one can identify the isolated bacteria based on a DNA fingerprint[1,4] following its confinement. In addition, the orientation of the vancomycin probe on the surface and the exact functional groups that are targeted in the chemical binding of the probe molecule to the nanoparticle surface (*i.e.*, the architecture of the vancomycin on the nanoparticle surface) are far easier to control than in the case of antibodies. We recently reported the synthesis of these vancomycin-modified silica encapsulated iron oxide nanoparticles in a previous report.[22] Briefly, the nanoparticles were prepared by first coating a commercially available iron oxide nanoparticle (EMG 304 ferrofluid, Ferrotec Corporation) with silica (**SNP**),[22−24] followed by modification of the resulting silica surface with 3-aminopropyldiethoxymethyl silane, generating an amine-modified **SNP** (**1-SNP**).[22] These amine-modified nanoparticles can be quantitatively converted to carboxylic acid terminated nanoparticles, **2-SNP**, through reaction with succinic anhydride in dry DMF. Both **1-SNP** and **2-SNP** have diameters of ~50 nm. This investigation was also extended to include a series of commonly utilized and commercially available particles that were purchased from Dynal Biotech Inc. and modified with vancomycin. These particles were 2.8 μm in diameter and terminated with either amine groups (**1-Dynal$_{2.8}$**) or carboxylic acid groups (**2-Dynal$_{2.8}$**) or 1.0 μm in diameter and terminated with carboxylic acid groups (**2-Dynal$_{1.0}$**). A comparison between Dynal beads and the SNPs that we have prepared is necessary because Dynal beads are a popular choice for magneto-immunocapture assays.[25] As such, it is impor-

tant to compare and contrast the differences in the magnetic confinement of the bacteria mediated by these particles. As highlighted above, vancomycin has two individually addressable functional groups, so it can be anchored to the surface of particles in distinct orientations with distinct architectures (Scheme 1). That is, amide bonds can be generated between an amine-modified particle (**1-SNP** and **1-Dynal$_{2.8}$**) and the carboxylic acid group of vancomycin to generate **3-SNP** and **3-Dynal$_{2.8}$** (Scheme 1A). Conversely, the carboxylic acid groups of **2-SNP**, **2-Dynal$_{1.0}$**, and **2-Dynal$_{2.8}$** can be reacted with 1-ethyl-3-[3-dimethylaminopropyl]carbodiimide hydrochloride (EDC) and *N*-hydroxysuccinimide (NHS) to yield the NHS ester-modified particles, **2(NHS)-SNP**, **2(NHS)-Dynal$_{1.0}$**, and **2(NHS)-Dynal$_{2.8}$**, respectively, which are subsequently reacted with the primary vancosamine nitrogen of vancomycin to yield **4-SNP**, **4-Dynal$_{1.0}$**, and **4-Dynal$_{2.8}$**, respectively (Scheme 1B). Here, the orientation of the vancomycin molecule is essentially flipped 90° on the surface of the particle. Vancomycin can also be modified with linkers prior to attachment to the particle surface (vancomycin-PEG and vancomycin-C4), in order to extend it from the particle surface as depicted in Scheme 1C for **3(PEG)-SNP**, **3(PEG)-Dynal$_{1.0}$**, and **3(C4)-Dynal$_{1.0}$**. This allows us to probe if the added flexibility of the butyl (C4) or diethylene glycol (PEG) spacer allows the vancomycin molecule to adopt orientations better suited for interactions with the surface of the pathogen. Previously, other groups have utilized the carboxylic acid group exclusively (similar to **3-SNP**, Scheme 1) to anchor vancomycin molecules to the surface of 3 nm FePt[5] and 10 nm Fe_3O_4 nanoparticles[6] and were able to magnetically confine a series of pathogens. However, it has yet to be reported how the magnetic confinement of pathogens will be affected by (1) changes in the orientation/architecture of the vancomycin molecule, (2) the distance between the vancomycin moiety and the particle surface or (3) the size of the particle supporting the vancomycin molecule, and the relative ligand surface coverage on the nanoparticles where these factors are expected to affect the specific interactions between the probe and the pathogen surface and thus the magnetic confinement of the pathogens.

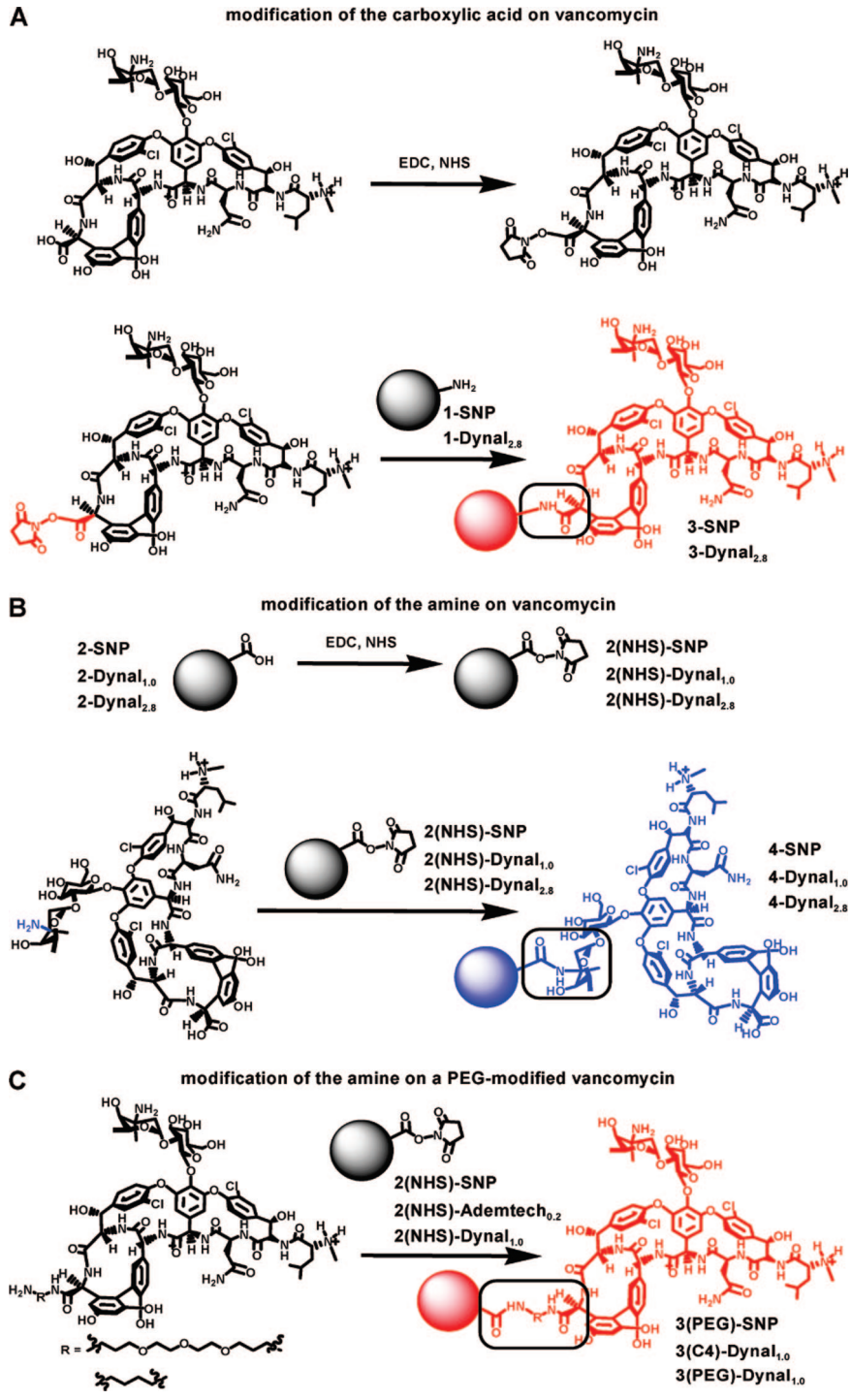

Scheme 1. The general reaction scheme employed to prepare the vancomycin-modified particles. The modification site in the vancomycin molecule is highlighted with a box in each reaction product.

Orientation/Architecture Effects on the Magnetic Confinement of Pathogens. We first investigated how changes in the orientation/architecture of vancomycin (**3-SNP** *vs* **4-SNP**) affected the affinity capture of a variety of both Gram-positive (denoted with (+)) and Gram-negative (denoted with (−)) bacteria. Note that vancomycin is

only expected to bind to Gram-positive bacteria *via* selective H-bonding interactions between its heptapeptide backbone and the D-alanyl-D-alanine groups of the cell wall (Figure 1).[18] Gram-negative pathogens have an additional outer membrane that covers much of the cell surface. This membrane is highly impenetrable to vancomycin, restricting access to the D-alanyl-D-alanine groups. As a result, Gram-negative pathogens are normally not susceptible to vancomycin.[26,27] The BSA-blocked vancomycin-modified nanoparticles (**3-SNP** or **4-SNP**, 1×10^{11} particles) in 100 μL of MES buffered water (pH = 6, [NaCl] = 100 mM) were spiked with a species of Gram-positive (+) or Gram-negative (−) bacteria, namely *E. coli* (−), *E. faecalis* (+) or *S. epidermidis* (+) (30−300 cfu in 25 μL of MES buffer, [NaCl] = 100 mM) and incubated for 2 h. Following incubation, the resulting **3-SNP** or **4-SNP**-labeled bacteria were magnetically confined for one hour at which time the supernatant was removed and the confined nanoparticle−bacteria conjugates were redispersed in 25 μL of MES buffered water. The number of bacteria magnetically isolated by **3-SNP** or **4-SNP** were then determined *via* plate counting of the isolated nanoparticle−pathogen conjugates. To ensure that all of the bacteria employed in the experiment were accounted for, the supernatant was also plate counted to ensure that the total number of bacteria recovered was consistent with the number originally utilized in the magnetic capture experiment. Though this plate-counting technique was employed for the majority of the experiments highlighted in this report, we also monitored the magnetic confinement of the pathogens with fluorescently labeled bacteria *(E. coli* and *S. aureus*). In these cases, the capture efficiency was monitored as a function of the fluorescence emission intensity, where the fluorescence emission intensity of a bacteria-spiked solution without addition of the nanoparticle was compared to the emission intensity of an identical bacteria-spiked solution following incubation and magnetic confinement with a vancomycin-modified nanoparticle (see Supporting Information). Note that the magnetic capture efficiencies presented are the result of plate counting analysis unless otherwise stated.

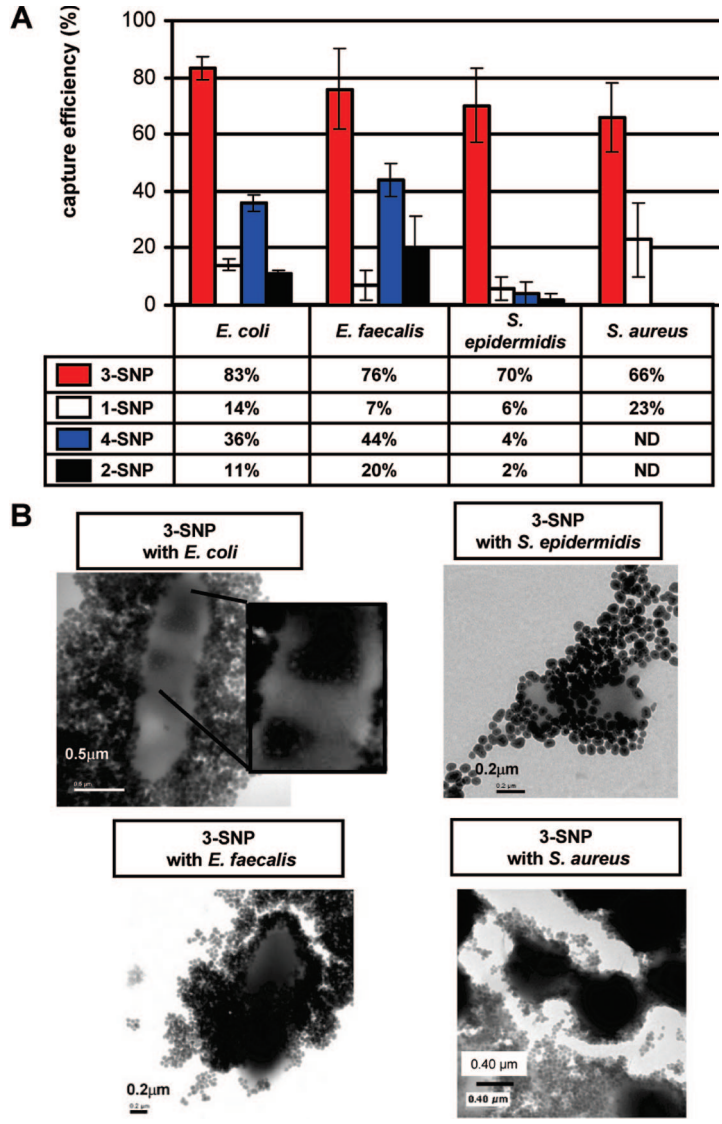

Figure 2. Bar graphs representing the magnetic capture efficiency *E. coli*, *E. faecalis*, *S. aureus*, and *S. epidermidis* by 3-SNP, 1-SNP (control nanoparticle terminated with an amine), 4-SNP, and 2-SNP (control nanoparticle terminated with a carboxylic acid) (A) and the TEM images of the 3-SNP-pathogen conjugates for *E. coli*, *E. faecalis*, *S. aureus*, and *S. epidermidis* (B). The capture efficiencies reported are the average of least three replicates for each bacteria.

The results of the magnetic capture assays for **3-SNP** and **4-SNP** are provided in Figure 2, where the bar graphs represent the percentage of pathogen magnetically confined during the experiments. It is clear from the data in Figure 2 that the capture efficiency is strongly dependent on the orientation/architecture of the vancomycin moiety on the surface of the SNP for all bacteria investigated. This is analogous to the results we recently reported with respect to magnetically confining vancomycin antibody-modified polystyrene beads.[22] A large excess of **3-SNP** or **4-SNP** *versus* bacteria was utilized in all of these experiments (1×10^8 to 1×10^9 fold excess nanoparticle). Though determining the lowest concentration of bacteria cells we could confine was not a priority, we were easily able to isolate

300 cells/mL for *E.coli*, *E. faecalis*, and *S. epidermidis* strains of bacteria. Vancomycin itself is well-known to inhibit the growth of Gram-positive bacteria at concentrations of 2 μg/mL.[28] To ensure that plate counting is a valid technique to characterize the magnetic confinement efficiency of these bacteria, **3-SNP** (1×10^{11} and 1×10^{12} nanoparticles) were incubated with ~1000 cfu of *S. aureus* for 2 h and then cultured on a standard BHI plate. This experiment verified that the **3-SNP** used in this experiment did not have vancomycin concentrations high enough to inhibit the growth of *S. aureus*, verifying that plate counting is a valid technique for the characterization of the magnetic confinement of the bacteria. In fact, we can roughly calculate the concentration of vancomycin in these solutions because we know that there are ~10 vancomycin molecules/**3-SNP**. As such, this translates to ~0.02 and 0.2 μg/mL for **3-SNP** concentrations of 1×10^{11} and 1×10^{12}, respectively. It should be noted that at significantly higher concentrations (2−4 μg/mL), Gu and co-workers reported that 5 nm vancomycin-modified gold nanoparticles can inhibit the growth of a number of both Gram-positive and Gram-negative bacteria.[28] Though we were unable to anchor significantly more vancomycin to the surface of the nanoparticles by changing the relative ratios of reagents (EDC, NHS, and vancomycin) and the solvents in which the reactions were carried out, we were satisfied with that fact that this surface coverage was not inhibitory to bacteria growth and allowed us to utilize plate counting for analysis.

Surprisingly, **3-SNP**, and to a lesser extent **4-SNP**, were able to capture Gram-negative bacteria, despite the outer membrane impeding the interaction between the vancomycin molecule and the D-alanyl-D-alanine groups on the bacterial surface. This is, however, consistent with recent reports by both Gu *et. al*[5] and Lin *et al*.[6] Gu *et. al* speculate that the ability for the vancomycin-modified nanoparticles to capture the *E. coli* could be due to either unspecific binding between receptors on the pathogen surface and the glycosides on the vancomycin moiety or breaks/deformities in the outer membrane of the Gram-negative bacteria exposing D-alanyl-D-alanine groups on the interior bacterial surface.[5] Our data suggest that either of these proposals could be valid. That is, the glycosides (disaccharides) are free to interact with the bacterial surface in **3-SNP**, whereas they are at least partially blocked in **4-SNP** because vancomycin is anchored to the nanoparticle surface through the primary amine on the disaccharide group. However, it is interesting to note that the TEM images published by Gu *et al*.[5] as well our TEM images reveal that that the distribution of **3-SNP** on the surface of the Gram-negative bacteria was often patchy while, in general, the coverage is more evenly distributed on Gram-positive bacteria, particularly on *S. epidermidis* and *S. aureus* (Figure 2B and the Supporting Information). We speculate that these common patchy regions may reflect thinner outer membrane zones exposing the peptidoglycan cell wall while outer membrane synthesis is under way. This is yet to be proven, however. Control experiments carried out with the unmodified nanoparticles (*i.e*., **1-SNP** and **2-SNP**, which have amine and carboxylic acid groups, respectively) suggest that the interaction between the SNPs and the bacteria cell surface is mediated through specific interactions between the vancomycin on the nanoparticle (**3-SNP** and **4-SNP**) and receptors on the surface of the bacteria, rather than nonspecific interactions between any remaining amine or carboxylic acid groups on the vancomycin-modified nanoparticles. We also acquired TEM images of **1-SNP** and **2-SNP** following incubation with *E. coli* and *S. aureus* cells, and there is significantly less interaction between the unmodified nanoparticles and the bacteria cells than is the case when **3-SNP** is incubated with the cells (see Supporting Information). We also carried out microagglutination assays[29] on **1**, **2**, **3**, and **4-SNP** with *S. aureus*, a Gram-positive species of bacteria. Microagglutination assays are clumping assays carried out in a microtiter plate that take advantage of complementary interactions between multivalent targets, in this case between the numerous D-alanyl-D-alanine receptors on the surface of the bacteria and the multiple vancomycin probes anchored to the surface of the nanoparticles (**3-SNP** and **4-SNP**). Within these assays, multivalent interactions between the nanoparticles and the bacteria result in a clumping or aggregation. This aggregation can be visualized by a diffused cell morphology in the microtiter wells. Weak interaction between the nanoparticles and the bacteria are characterized by the precipitation of the bacteria into a pellet at the bottom of the microtiter wells. The relative strength of the interactions can be elucidated by incubating a constant number of bacteria cells with 2-fold dilutions of either **1**, **2**, **3**, or **4-SNP**. As highlighted in Figure 3, only **3-SNP** shows a diffuse cell morphology in the microagglutination experiment (wells

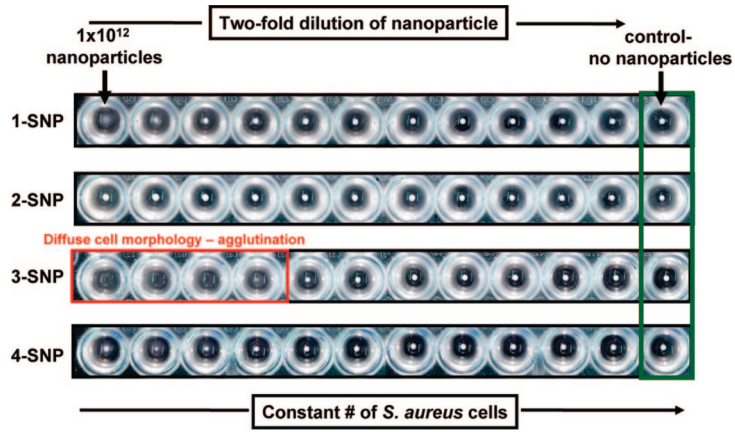

Figure 3. A microagglutination assay for *S. aureus* cells incubated with 1-, 2-, 3-, and 4-SNP. Note that only 3-SNP displays the diffuse cell morphology expected for an efficient, multivalent interaction between many nanoparticles and many bacteria.

1−4). This suggests that **3-SNP** interacts with the *S. aureus* cells at least eight times more effectively than **4-SNP** and the control nanoparticles **1** and **2-SNP**, which all show very weak interactions with *S. aureus*, characterized by a "pellet" of unclumped bacterial cell at the bottom of the well at all concentrations investigated. It should be noted that **1-SNP** interacts somewhat in well 1, evidenced by a mixture of diffuse and pelleted cells. These results are fully consistent with the capture assay results described earlier and provide further evidence that **3-SNP** interacts with the bacteria surface more effectively than **4-SNP**.

It is interesting that the geometry of the vancomycin moiety has such a dramatic effect on the pathogen capture efficiency. There are a variety of reasons that can explain these results. The decrease in capture efficiency may be due to differences in the orientation of the vancomycin moiety as it is anchored to the nanoparticle surface through the different functional groups. For example, binding the vancomycin moiety to the surface in the different geometries could orient the heptapeptide backbone responsible for the specific interaction with the bacteria in very different environments, introducing steric hindrances that impede efficient binding. Anchoring vancomycin to the particle through the vancosamine nitrogen (**4-SNP**) should allow the heptapeptide binding region of vancomycin to be presented parallel to the nanoparticle surface, allowing it to interact with the receptors on the pathogen surface more effectively. Conversely, linking it through the carboxylic acid group (**3-SNP**) may position the heptapeptide binding region perpendicular to the particle surface and hinder specific interactions with the bacterial surface. However, this trend was not found experimentally, suggesting that sterics are not causing the decreased capture efficiency mediated by **4-SNP**. A more plausible reason for the difference in capture efficiency is differences in the association constants (K_a) or dissociation constants (K_d) between **4-** and **3-**based particles and the D-alanyl-D-alanine dipeptide on the bacterial cell wall. Kannan et. al report that the K_a for derivatives similar to **4-SNP** binding to D-alanyl-D-alanine is at least ~3 to 4 times less than for derivatives similar to **3-SNP**.[30] These authors suggest that the decreased binding affinity could be related to the elimination of a charge-bearing primary amine on the disaccharide moiety in **4**-based vancomycin derivatives. The inability to protonate this site destabilizes the vancomycin binding pocket, resulting in a decrease in the binding constant between the vancomycin and the D-alanyl-D-alanine on the bacteria cell wall surface. Following the investigations with the **SNP**-based nanoparticles, a series of experiments was then carried out with larger particles (**3-Dynal$_{2.8}$**, **4-Dynal$_{2.8}$**, and **3-Dynal$_{1.0}$**) in order to examine what effect the particle size has on the magnetic capture efficiency for the bacterial cells. There are reports that suggest nanoparticles should be superior to micrometer-sized particles for labeling of a given substrate, because of their higher surface area to volume ratio, potentially faster interaction kinetics, and good interaction homogeneity (*i.e.*, the nanoparticles are colloidally stable).[5,31] However, there are also reports suggesting that if equal numbers of nanoparticles or larger Dynal beads are anchored to the same cell, the Dynal bead labeled cells will have superior magnetophoretic mobilities, and be confined more effectively.[32,33] As such, it is interesting to investigate, for example, how the particle coverage on the bacteria surface will affect the magnetic confinement of the bacteria, where there will be significantly more SPNs interacting with a bacteria than will be the case for the 1 μm Dynal bead. It should be noted that despite their rather large overall size, the superparamagnetic properties of the micrometer-sized Dynal particles are actually dictated by the large number of ferrite nanoparticles encapsulated within the particles.

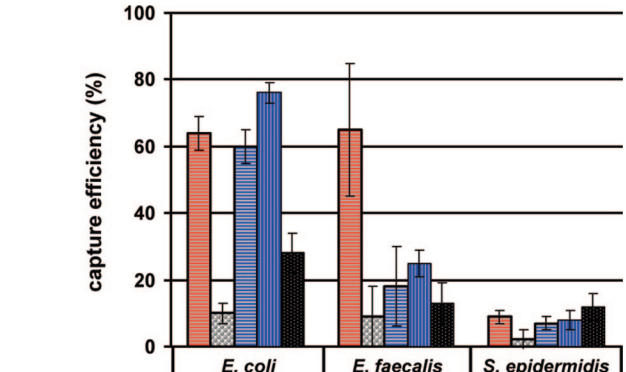

	E. coli	*E. faecalis*	*S. epidermidis*
3-Dynal$_{2.8}$	64%	65%	9%
1-Dynal$_{2.8}$	10%	9%	2%
4-Dynal$_{2.8}$	60%	18%	7%
4-Dynal$_{1.0}$	76%	25%	8%
2-Dynal$_{2.8}$	28%	13%	12%

Figure 4. Bar graphs representing the magnetic capture efficiency of *E. coli*, *E. faecalis*, and *S. epidermidis* by 3-Dynal$_{2.8}$, 1-Dynal$_{2.8}$ (control nanoparticle terminated with an amine), 4-Dynal$_{2.8}$, and 4-Dynal$_{1.0}$ and 2-Dynal$_{2.8}$ (control nanoparticle terminated with a carboxylic acid). The capture efficiencies reported for each species of bacteria are the average of least three replicates.

For these microparticles, the capture experiments were set up as described earlier, but different concentrations of particle were employed in each experiment. Here there were 3×10^7 **3-Dynal$_{1.0}$** particles or 1×10^7 **3-Dynal$_{2.8}$**, **4-Dynal$_{2.8}$** particles utilized to label and magnetically confine ~300 bacteria cells. In contrast to the results for **3-SNP** and **4-SNP**, as the size of the particle to which vancomycin is anchored increases from ~50 to 1000 and 2800 nm, respectively, there is no clear difference in the capture efficiency as the orientation/architecture of the substrate is altered (**3-Dynal$_{2.8}$**, **4-Dynal$_{2.8}$**, and **3-Dynal$_{1.0}$** in Figure 4) and the overall ability for these particles to confine the bacteria are

poor with respect to that for the **3-SNP**. Though these results could be due to a number of factors, we felt that the main problem could be due to a lack of mobility associated with the vancomycin molecule being anchored closely to the surfaces of the large particles. In the case of **3-Dynal$_{2.8}$**, **4-Dynal$_{2.8}$**, and **3-Dynal$_{1.0}$** there is no spacer group between the vancomycin substrate and the particle surface, in contrast to the situation on both **3-SNP** and **4-SNP**. As such, we felt that incorporating a spacer group between the particle surface and the vancomycin moiety may improve the mobility of the substrate, allowing it to more easily adopt orientations that mediate interactions between the heptapeptide backbone and receptors and the pathogen surface. It should also be noted that the amine and carboxylic acid-modified Dynal beads (**1-Dynal$_{2.8}$**, **2-Dynal$_{2.8}$**) cannot effectively confine the bacteria in the absence of vancomycin, suggesting the interactions between the nanoparticles and the bacteria are mediated by the vancomycin moiety (Figure 4).

Effects of Linker Incorporation on the Magnetic Confinement of Pathogens. In the case of **3-SNP**, vancomycin is anchored close to the surface of the nanoparticle surface with a short linker of three methylene units (through 3-aminopropyldiethoxymethyl silane). We chose to incorporate both a four-carbon spacer (C4) and a diethylene glycol spacer (PEG) between the particle surface and vancomycin. This allows us to prepare a vancomycin derivative that remained water soluble (a characteristic essential for aqueous surface modification of the particles) and investigate how extending the probe increasing further from the surface will affect the pathogen capture efficiency. The PEG spacer may also find utility in preventing nonspecific absorption between the nanoparticles and biomolecules, which will be useful if the vancomycin-modified particles are to be employed in a pathogen capture from a biological medium such as blood or a food-based sample. With respect to the ~50 nm SNPs, the addition of a PEG spacer [(**3-SNP** (3-atom spacer) *vs* **3**(**PEG**)-**SNP** (13-atom spacer)] neither hinders, nor helps the capture efficiency of the *E. coli* (−), *E. faecalis* (+), and *S. epidermidis* (+) by the vancomycin-modified particles, and the capture efficiency remains high for all pathogens confined in the investigation (Supporting Information). However, incorporating a shorter linker between the Dynal bead and vancomycin (four atoms, **3**(**C4**)-**Dynal$_{1.0}$**) does not allow for consistent confinement of the entire series of Gram-positive pathogens investigated. Only when the spacer length is very long (13 atoms, **3**(**PEG**)-**Dynal$_{1.0}$**) is the confinement efficiency for the large particles consistent for the entire series of Gram-positive bacteria (*i.e.*, *E. faecalis*, *S. epidermidis*, and *S. aureus*), as it is for **3-SNP** and **3**(**PEG**)-**SNP**. This data is highlighted in Figure 5. That is, only when the long PEG linker separates vancomycin from the surface of the Dynal bead is the capture of Gram-positive bacteria both efficient and consistent for the entire range of bacteria investigated, presumably because the added flexibility allows the heptapeptide backbone to adopt orientations better suited for effective interactions with bacterial surface ligands. It should be noted that the vancomycin moiety is actually extended four carbons further from the surface in **4-SNP** than it is in **3-SNP**, and it does not function as well, despite the fact that it should have some additional flexibility. As such, we chose to not pursue this geometry any further. Again we tested the antibiotic activity of the **3**(**PEG**)-**Dynal$_{1.0}$** particles to ensure that plate counting was a valid method for determining the capture efficiency of the bacteria and incubation of *S. aureus* cells with 1×10^6 and 1×10^7 **3**(**PEG**)-**Dynal$_{1.0}$** (corresponding to 4×10^{-2} and 0.4 μg/mL of vancomycin) does not inhibit bacterial cell growth (see Supporting Information).

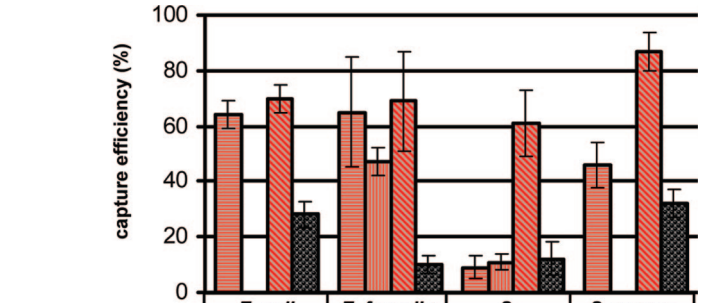

	E. coli	E. faecalis	S. epidermidis	S. aureus
3-Dynal$_{2.8}$	64%	65%	9%	46%
3(C4)-Dynal$_{1.0}$	ND	47%	11%	ND
3(PEG)-Dynal$_{1.0}$	70%	69%	61%	87%
2-Dynal$_{1.0}$	28%	10%	12%	31%

Figure 5. Bar graphs representing the magnetic capture efficiency *E. coli*, *E. faecalis*, *S. epidermidis*, and *S. aureus* by 3-Dynal$_{2.8}$, 3(C4)-Dynal$_{1.0}$, 3(PEG)-Dynal$_{1.0}$, and 2-Dynal$_{1.0}$ (control nanoparticle terminated with a carboxylic acid). The capture efficiencies reported for each species of bacteria are the average of least three replicates.

In reviewing the characteristics of the labeling of the bacterial cells and the subsequent magnetic confinement for both **3-SNP** and **3**(**PEG**)-**Dynal$_{1.0}$**, there are a number of interesting differences. First, we determined that the incubation time required for sufficient bacteria cell labeling to yield efficient capture of the bacterial cells with **3**(**PEG**)-**Dynal$_{1.0}$** was much shorter that that for the **3-SNP**-based nanoparticles (15 min *vs* 30−60 min, see Supporting Information). This is likely the result of drastically different surface coverages of vancomycin on the two sets of nanoparticles. Because there are only between 9 and 12 vancomycin molecules on the surface of the **3-SNP**, it is unlikely that there are only one or two interactions between the nanoparticle and the bacteria cell wall. Though we were not able to significantly increase the number of vancomycin molecules on the surface of the **3-SNP** despite changing the synthetic conditions employed in the synthesis (generally get surface coverages of 0.0015 vancomycin/nm^2), we were able to functionalize the surface of **3**(**PEG**)-**Dynal$_{1.0}$** with significantly higher concentra-

tions of vancomycin (0.5 vancomycin/nm^2). This increased surface coverage of vancomycin on the nanoparticle surface may contribute to the decreased incubation times required for efficient confinement, because multivalent attachment of **3**(**PEG**)-**Dynal$_{1.0}$** would have a high probability of occurring, resulting in stronger, faster binding of the particle to the bacteria surface. These results are supported by a report by Sundram and Griffin[21] who suggest that vancomycin dimers show enhanced binding affinities to Gram-positive cells in comparison to vancomycin monomers and also by Gu and co-workers who reported an incubation time of 10 min was sufficient to densely label a variety of bacteria with vancomycin-modified FePt nanoparticles.[5] Second, the confinement time for the Dynal beads is significantly faster than that required for the magnetic confinement mediated by **3-SNP** (>5 min *vs* 30 min). This is related to the high loading of superparamagnetic material into the Dynal beads (~37% by mass ferrites for **2-Dynal$_{1.0}$**), whereas the SNPs have only one to three superparamagnetic nanoparticles encapsulated within the silica shell. As such, the magnetic confinement of the resulting Dynal bead-labeled bacteria is superior to that for the SNP-labeled bacteria. Finally, another inherent difference between the Dynal bead-bacteria conjugates and the **3-SNP**-bacteria conjugates is the relative number of particles than can be accommodated around a given bacterial cell. In contrast to the ~50 nm **3-SNPs** which cover a significant portion of the entire surface of the bacteria (Figure 2 and Supporting Information), the large diameter of the **3**(**PEG**)-**Dynal$_{1.0}$** and **3-Dynal$_{2.8}$** will limit the number of particles interacting with the bacteria. In fact, the TEM images suggest that there are actually several bacteria interacting with a single **3**(**PEG**)-**Dynal$_{1.0}$** (Figure 6A and B) in contrast to the situation with **3-SNP**. Moreover, the specific interaction with the bacteria appears to aggregate **3**(**PEG**)-**Dynal$_{1.0}$**, whereas nonspecific interactions between the unmodified **2-Dynal$_{1.0}$** does not result in efficient interaction and hence there is no aggregation between the bead and the bacteria (Figure 6C and D). Because of their large size relative to the bacteria, we expected to see many bacteria surrounding the **3-Dynal$_{2.8}$**-based particles in the TEM images of the bead-bacteria conjugates. However, there was consistently only one or two *S. aureus* cells interacting with the beads and there were essentially no Dynal bead-bacteria aggregates similar to those found with **3**(**PEG**)-**Dynal$_{1.0}$** (see Supporting Information). This is a nice confirmation supporting our magnetic confinement/plate counting results suggesting that **3-Dynal$_{2.8}$**-based beads cannot interact with the bacteria as effectively as **3**(**PEG**)-**Dynal$_{1.0}$**. Finally, because the bacteria actually assemble around the Dynal beads, significantly smaller excesses of **3-Dynal$_{2.8}$** and **3**(**PEG**)-**Dynal$_{1.0}$** (1×10^2 to 1×10^5) can be employed in the magnetic confinement experiments in contrast to the larger excesses employed with **3-SNP**-based nanoparticles (1×10^6 to 1×10^9). This analysis highlights the importance of combining both TEM results and the capture data because TEM provides only a snapshot of what is occurring between the particles and the bacteria in the solid state. It is quite necessary to acquire both the magnetic capture data and couple it to the information in the TEM images to provide the best overall evaluation of the various nanoparticles abilities to participate in affinity capture experiments for bacteria. Again, it should be noted that the unmodified carboxylic acid-modified Dynal beads (**2-Dynal$_{1.0}$**) cannot effectively confine the bacteria, suggesting the interactions between the nanoparticles and the bacteria are mediated by the vancomycin moiety anchored to the particle surface (Figure 5).

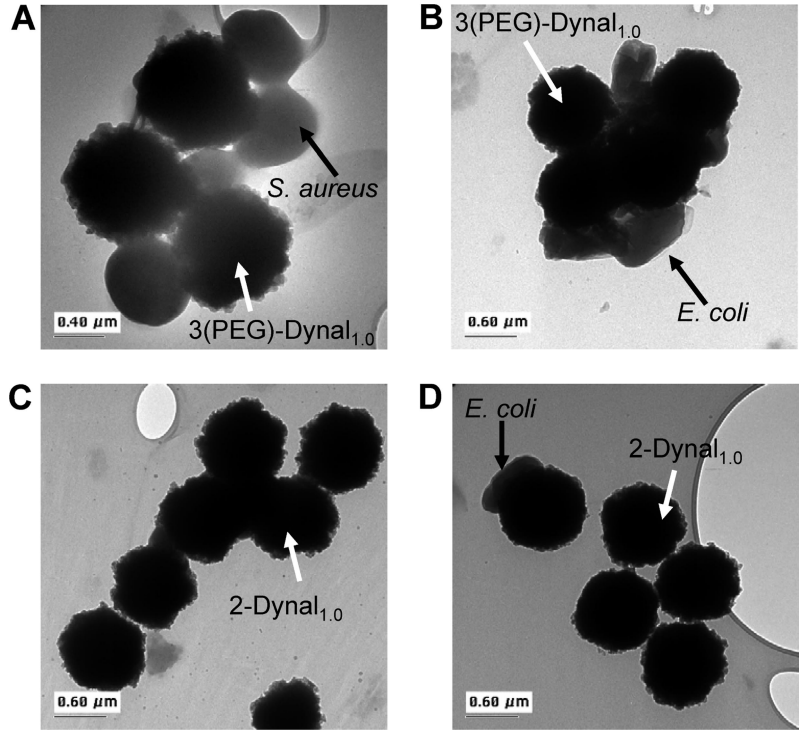

Figure 6. TEM images of the 3(PEG)-Dynal$_{1.0}$ pathogen conjugates for, *S. aureus* (A) and *E. coli* (B) as well as the corresponding control beads (2-Dynal$_{1.0}$) for *S. aureus* (C) and *E. coli* (D). Note that the conjugates are aggregated when the Dynal beads are modified with vancomycin.

Because our interests lie in the development of nanoparticle-based probes for confining several patho-

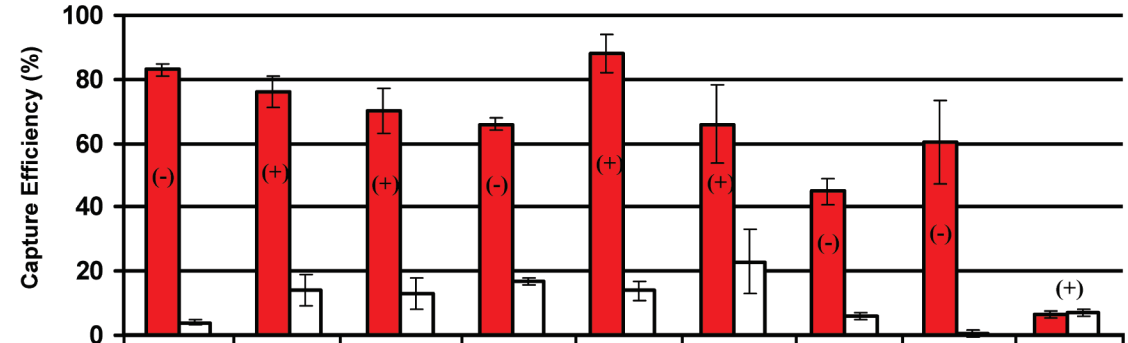

	E. coli	E. faecalis	S. epidermidis	P. aeruginosa	S. agalactiae	S. aureus	K. oxytoca	S. maltophilia	E. faecium (VRE)
3-SNP	83%	76%	70%	66%	88%	66%	45%	60%	7%
1-SNP	4%	14%	13%	16%	14%	23%	4%	1%	7%

Figure 7. Bar graphs representing the magnetic confinement efficiency for the magnetic capture of a variety of Gram-positive (+) and Gram-negative (−) by 3-SNP (A). The capture efficiencies reported are the average of least three replicates each of the bacteria.

gens that can later be identified by a genomic DNA fingerprint,[3,4] we chose to extend the investigation of **3-SNP** to a large series of pathogens in order to learn the range of different species that could be magnetically confined with a single nanoparticle probe. As highlighted in Figure 7, **3-SNP** has the ability to efficiently confine at least eight different species of Gram-positive and Gram-negative bacteria, though the nanoparticles are incapable of interacting with and confining vancomycin-resistant *enterococci* (VRE, Figure 7). A frequent difference between vancomycin-susceptible and vancomycin-resistant strains of bacteria is the substitution of the terminal D-alanyl-D-alanine dipeptide for a D-alanyl-D-lactate dipeptide on the pathogen surface (conferred by the VanA resistance gene).[18] This results in the loss of one hydrogen bond and the introduction of a lone pair−lone pair repulsion that greatly increases the dissociation constant of the interaction.[34,35] The low capture efficiency suggests that the nanoparticles do not interact effectively with this species of pathogen, which is to be expected considering the D-alanyl-D-alanine dipeptide receptor has been altered on the bacteria cell wall surface. Gu and co-workers recently demonstrated that small gold and FePt-based nanoparticles decorated with ~10−31 vancomycin molecules can interact with and, in the latter case, actually magnetically confine VRE.[5,28] This effective interaction is attributed to the ability for the surface-bound vancomycin moieties to multivalently interact with the surface of the bacteria. In fact, the activity of vancomycin dimers in the inhibition of VREs is rationalized with a similar argument (*i.e.*, strong multivalent interaction).[21] The poor magnetic confinement mediated by **3-SNP** in regards to the VRE is likely due to the inability for the small number of vancomycin moieties on its surface to interact multivalently with the D-alanyl-D-lactate dipeptide receptors on the surface of the bacteria. In the absence of this strong interaction, **3-SNP** cannot mediate an effective confinement of these bacteria. Finally, the stability of

TABLE 1. The Magnetic Capture Efficiency of *E. coli*, *E. faecalis*, and *S. epidermidis* by 3-SNP Measured over 112 Days

	E. coli % capture	*E. faecalis* % capture	*S. epidermidis* % capture
day 1	112	100	83
day 8	94 (83%)[a]	79 (79%)[a]	85 (102%)[a]
day 64	57 (51%)[a]	72 (72%)[a]	89 (107%)[a]
day 94	82 (73%)[a]	66 (66%)[a]	25 (29%)[a]
day 112	58 (52%)[a]	81 (81%)[a]	25 (31%)[a]

[a]Note: (a) the values in parentheses for day 8-day 112 represent the capture efficiency for that particular day relative to that on Day 1. Capture efficiencies of 100% or more can be explained by the intrinsic variation involved in the plate counting method.

3-SNP is similar to what would be expected for most antibody-modified magnetic particles. That is, **3-SNP** nanoparticles retain reasonable affinity capture activity for 3 months with storage in MES buffer at 4 °C (Table 1). The intrinsic variation involved in plate counting method is generally below 10%. For day 94 measures, replicates of plate counts showed greater than expected variations, therefore indicating possible methodological mishaps. This does not change the general conclusion that reasonable capture efficiency can be maintained for two months for the three bacterial species tested, and up to three 3 months for *E. faecalis*.

CONCLUSIONS

We have demonstrated the power of incorporating small molecule probe-modified nanoparticles into a magnetic capture assay for multiple Gram-positive and Gram-negative bacteria and illustrated how easily the orientation/architecture of the probe can be controlled as it is anchored to particle surfaces. The ability to control the architecture is important because only one of two architectures leads to the efficient confinement of bacteria by small (~50 nm) nanoparticles. We have also demonstrated that the surface coverage of vancomcyin plays an important role in the time required for ef-

ficient labeling to the bacteria with the magnetic particles (15 *vs* 30−60 min as the surface coverage increases), and that it is necessary to extend the probe from the surface of the larger nanoparticles with a diethylene glycol spacer in order to impart more flexibility to the ligand, presumably allowing it to adopt orientations more amenable to effective interactions with pathogen surface ligands. Importantly, the time required for pathogen capture can be significantly decreased when the larger, highly loaded nanoparticles are employed for bacterial cell capture (<5 min rather than 30−60 min). Together these results demonstrate that small molecule probes are excellent alternatives to antibodies for use in nanoparticle-based cell labeling and magnetic capture assays, where the temperature, long-term stability, reaction conditions used for surface modification and ability to control the surface architecture/orientation are significantly more flexible than those for typical antibody-based strategies. Finally, we also show that a single small-molecule modified nanoparticle can be utilized to target and isolate many different pathogens, negating the need to prepare specific nanoparticles to target and isolate specific pathogens.

METHODS

Water-soluble iron oxide nanoparticles (Fe_xO_y) were obtained from Ferrotec Corporation (average diameter 10 nm, EMG 304 ferrofluid). Tetraethoxysilane (TEOS) and 3-aminopropyldiethoxymethylsilane (APDEMS) were both ordered from Gelest, Inc. Ammonium hydroxide (NH_4OH, 28−30 wt %), high purity 2-propanol, dimethylsulfoxide (DMSO), dimethylformamide (DMF), and dichloromethane were obtained from EMD Chemicals, Inc. *N*-(3-dimethylaminopropyl)-*N*′-ethylcarbodiimide hydrochloride (EDC), diisopropylethylamine, *N*-hydroxy succinimide (NHS), 1-hydroxybenzotriazole (HOBT), *N,N,N*′,*N*′-tetramethyl-*O*-(1*H*-benzotriazol-1-yl)uronium hexafluorophosphate (HBTU), vancomycin, 1,4-diaminobutane, 4,7,10-trioxa-1,13-tridecanediamine, and MES were purchased from Aldrich and used without further purification. The carboxylic acid and amine modified Dynal beads (**1-Dynal$_{2.8}$**, **2-Dynal$_{2.8}$**, and **2-Dynal$_{1.0}$**) were purchased through Invitrogen. Water was purified with a Millipore Q-guard 2 purification system (Millipore Corporation). Only purified water was used in the experiments. Fluorescent bacteria were purchased from Molecular Probes.

The vancomycin derivatives were purified by RP-preparative HPLC on a Waters Delta Prep 4000 system, equipped with a Waters 996 photodiode detector and a Zorbax 300SB-C18 column. Analytical RP-HPLC was performed with an Agilent 1100 series HPLC employing a Zorbax 300SB-C18 column (5 μm) with dimensions of 4.6 mm × 150 mm.

Transmission electron microscopy (TEM) was used to characterize the various Fe_xO_y@SiO_2 based core−shell nanoparticles. The TEM images were obtained using a Philips CM20 FEG microscope operating at 200 kV. The SEM images were acquired on a JEOL model JSM-5300 microscope. Samples were prepared by dropcasting several drops of the particle dispersion onto 200 mesh copper/holey carbon TEM grids with a pipet.

Preparation of 1-SNP, 2-SNP, 3-SNP, and 4-SNP. The preparation and characterization of these nanoparticles has previously been reported by Kell and Simard.[22] This report elucidated that **3-SNP and 4-SNP** contain 9 and 12 vancomycin molecules per nanoparticle, respectively. Following preparation, the nanoparticles were incubated in a 0.1% solution of BSA in MES overnight, centrifuged, and redispersed in 30 mM MES buffer.

Synthesis of NH_2−C4-Vancomycin. The preparation of NH_2−C4-vancomycin was carried out through a process developed by Sundram.[21] Vancomycin (100 mg, 6.8×10^{-5} mol) was dissolved in 2 mL of DMSO. To this was added 1,4-diaminobutane (30 mg, 3.4×10^{-4} mol) in 2 mL of DMF. The mixture was cooled in an ice bath, and HBTU (38 mg, 1.0×10^{-4} mol) and HOBT (13.2 mg, 1.0×10^{-4} mol) were added as 1 mL solutions in DMF. Finally, diisopropylethylamine (20 μL, 11.4×10^{-4} mol) was added, and the mixture was stirred overnight. The product was precipitated with dichloromethane and centrifuged to isolate the white product. The precipitate was dissolved in 3 mL of Millipore water and purified *via* preparative reverse-phase HPLC (5−40% water/acetonitrile with 0.1% TFA over 20 min, $R_f = 12.3$ min). The product was characterized by HPLC (>90% by area) and mass spectrometry. The MS exhibited an ion of ($M^+ + H$) $m/z = 1517$ (m/z (calcd) = 1517), consistent with a molecular ion of $[C_{70}H_{85}Cl_2N_{11}O_{23}]^+$.

Synthesis of NH_2−PEG−Vancomycin. The reaction was carried out as described above, except 4,7,10-trioxa-1,13-tridecanediamine (75 mg, 3.4×10^{-4} mol) was used in place of 1,4-diaminobutane. The precipitate was dissolved in 3 mL of Millipore water and purified *via* preparative reverse-phase HPLC (5−40% water/acetonitrile with 0.1% TFA over 20 min, $R_f = 9.2$ min). The product was characterized by HPLC (>90% by area) and mass spectrometry. The MS exhibited an ion of ($M^+ + H$) $m/z = 1651$ (m/z (calcd) = 1650), consistent with a molecular ion of $[C_{76}H_{97}Cl_2N_{11}O_{26}]^+$.

Preparation of 3(PEG)-SNP. The carboxylic acid-modified nanoparticle (**2-SNP**) (10 mL, 1×10^{13} particles/mL) in 30 mM MES buffer was charged with 2 mg EDC and 2 mg NHS and mixed for 30 min at room temperature to generate the *N*-hydroxysuccinimidyl ester-modified nanoparticle (**2**(**NHS**)**-SNP**) *in situ*. The solution was then charged with 1 mg of NH_2−PEG-vancomycin and stirred for 12 h at room temperature. The resulting **3**(**PEG**)**-SNP** was centrifuged and unreacted NH_2−PEG−vancomycin was washed away with 5 mL MES buffer four times and finally dispersed in 8 mL MES and stored in the fridge at 4 °C.

Preparation of 4-Dynal$_{1.0}$ and 4-Dynal$_{2.8}$. The carboxylic acid modified nanoparticle (**2-Dynal$_{1.0}$**, 250 μL, 3×10^8 particles) was transferred to a glass vial and magnetically confined and redispersed in 250 μL of fresh MES buffer five times. The dispersion of **2-Dynal$_{1.0}$** was then spiked with 50 μL of a 50 mg/mL solution of EDC and 50 μL of a 50 mg/mL solution of NHS and stirred for ∼45 min. Following mixing, the nanoparticles were again magnetically confined and washed with fresh MES buffer (250 μL), redispersed in DMF (250 μL) and 50−750 μg of vancomycin was added. This solution was mixed for at least eight hours and the resulting **4-Dynal$_{1.0}$** was purified *via* sequential magnetic confinement and washing cycles (at least five) and dispersed in 1 mL of MES buffer. The same protocol was utilized in the synthesis of **4-Dynal$_{2.8}$** from **2-Dynal$_{2.8}$** (5×10^7 particles), but the functionalized nanoparticles were finally dispersed to 1×10^8 particles/mL. Note: there was no difference in the ability for **4-Dynal$_{1.0}$** and **4-Dynal$_{2.8}$** to confine pathogens when 0.05−0.75 mg was employed in the surface modification.

Preparation of 3(C4)-Dynal$_{1.0}$ and 3(PEG)-Dynal$_{1.0}$. The carboxylic acid modified nanoparticle (**2-Dynal$_{1.0}$**, 250 μL, 3×10^8 particles) was transferred to a glass vial and magnetically confined and redispersed in 250 μL of fresh MES buffer five times. The dispersion of **2-Dynal$_{1.0}$** was then spiked with 50 μL of a 50 mg/mL solution of EDC and 50 μL of a 50 mg/mL solution of NHS and stirred for ∼15 min. The solution was spiked with 0.5 mg of NH_2−C4-vancomycin and mixed for at least 8 h. Following mixing, the resulting **3**(**C4**)**-Dynal$_{1.0}$** nanoparticles were purified *via* sequential magnetic confinement and washing at least five times and finally dispersed in 1 mL of MES buffer. The same protocol was utilized in the synthesis of **3**(**PEG**)**-Dynal$_{1.0}$**, where 0.5 mg of this compound was also employed in the synthesis of the nanoparticle.

Preparation of 3-Dynal$_{2.8}$. The nanoparticle (**1-Dynal$_{2.8}$**, 250 μL, 3×10^8 particles) was transferred to a glass vial and magneti-

cally confined and redispersed in 250 μL of fresh MES buffer five times. The dispersion of **1-Dynal$_{2.8}$** was then spiked with 0.5 mg of vancomycin and allowed to stir for 15 min. Following 15 min, 50 μL of a 50 mg/mL solution of EDC and 50 μL of a 50 mg/mL solution of NHS were added and the resulting solution was vortex mixed for ~8 h. The resulting **3-Dynal$_{2.8}$** was purified *via* sequential magnetic confinement and washing cycles (5) and was then dispersed in 1 mL of MES buffer.

Isolation of Bacteria. The vancomycin-modified nanoparticles in 100 μL MES buffered water (pH = 6, [NaCl] = 100 mM) were spiked with a variety of both Gram-positive and Gram-negative pathogens (30−300 cfu in 25 μL of MES buffer). The nanoparticles were generally incubated for at least 1 h under gentle agitation using a rotary shaker in order to bind with the bacteria effectively. Shorter incubation times result in a less efficient magnetic confinement for some of the bacteria. The resulting nanoparticle−bacteria conjugates were magnetically confined for 1 h (**3-SNP** and **4-SNP**) or 5 min (**Dynal**-based nanoparticles) and the supernatant was carefully removed with a pipet. The magnetic confinement efficiency for each bacterium was determined *via* plate counting of the isolated nanoparticle−pathogen conjugates. This involved resuspension of the confined "pellet" of nanoparticle and bacteria in 25 μL of MES buffer and spread plating onto blood agar Petri dishes and subsequent growth during an overnight incubation at 37 °C. Recovered colony forming units were counted for both vancomycin-functionalized and the control nanoparticles, the latter used as nonspecific interaction controls. To ensure that all of the bacteria were accounted for, the supernatant was also spread plated onto blood agar Petri dishes and the total number of resulting cfu's from both the magnetically confined bacteria and the bacteria remaining in the supernatant was consistent with the total number of bacteria that was employed in the experiments. The ranges of excess particles for these experiments, defined as excess particles with respect to bacteria, are for **3-SNP** = 1×10^6 to 1×10^9, for **4-SNP** = 1×10^8 to 1×10^9, for **Dynal$_{2.8}$**-based particles = 1×10^2 to 1×10^5, and for **Dynal$_{1.0}$**-based particles = 1×10^2 to 1×10^5.

Growth of Cells for Antibiotic Susceptibility Studies. Vancomycin (2 μg), **3-SNP** (1×10^{11} and 1×10^{12} nanoparticles) and **3**(**PEG**)-**Dynal$_{1.0}$** (1×10^7 particles) were dispersed in 99 μL of MES buffered water and spiked with 1 μL of *S. aureus* cells (~1000 cells) and incubated for 2 h. The nanoparticle/bacteria or vancomycin/bacteria mixtures were then transferred to a brain/heart infusion plate (BHI plate), spread, and incubated at 37 °C overnight. The following morning the number of cfu's were counted and compared to a control sample where only the *S. aureus* cells were incubated in the absence of nanoparticles were cultured. The results are highlighted in the bar graphs in the Supporting Information, where the % viability is measured as the difference between the control and the bacteria mixed with the nanoparticles or vancomycin itself.

Microagglutination Analysis. Cell microagglutinations were performed essentially as described by Saito[29] and co-workers. Twofold dilutions of the nanoparticles were performed in MES buffered water (30 mM MES, pH 6.0, 70 mM NaCl) from wells 1−11 on a microtiter plate. Well 12 had only MES buffered water. The volume in each cell is 50 μL. One OD_{600} of *S. aureus* (~1×10^8 cells) was added to each well in a 50 μL aliquot bringing the total volume of the well to 100 μL. The plate was incubated overnight at 4 °C and photos were taken the following morning. Qualitatively, the minimum agglutination concentration (MAC) of **3-SNP** was determined to be ~1.125×10^{11} nanoparticles for 1×10^8 cells in 100 μL. None of the other nanoparticles showed MAC up to particle concentrations of 1×10^{12}/100 μL.

Acknowledgment. This work was financially supported by Genome Quebec and Genome Canada (grant 2005-064). We would like to thank Malgosia Daroszewska for assistance with HPLC, Catherine Bibby for acquiring some of the TEM images, Jim Margeson for acquiring the SEM images, and Jamshid Tanha (IBS) for discussions and advice during the course of this investigation.

Supporting Information Available: Additional experimental details and TEM images of the **3-SNP** and **Dynal** bead-bacteria conjugates and the control TEM for the various nanoparticles mixed with bacteria. This material is available free of charge *via* the Internet at http://pubs.acs.org.

REFERENCES AND NOTES

1. Picard, F. J.; Bergeron, M. G. Rapid Molecular Theranostics in Infectious Diseases. *Drug Discovery Today* **2002**, *7*, 1092–1101.
2. Kido, H.; Micic, M.; Smith, D.; Zoval, J.; Norton, J.; Madou, M. A Novel, Compact Disk-Like Centrifugal Microfluidics System for Cell Lysis and Sample Homogenization. *Colloids Surf., B* **2007**, *58*, 44–51.
3. Jia, G.; Siegrist, J.; Deng, C.; Zoval, J. V.; Stewart, G.; Peytavi, R.; Huletsky, A.; Bergeron, M. G.; Madou, M. J. A Low-Cost, Disposable Card for Rapid Polymerase Chain Reaction. *Colloids Surf., B* **2007**, *58*, 52–60.
4. Peytavi, R.; Raymond, F. R.; Gagne, D.; Picard, F. J.; Jia, G.; Zoval, J.; Madou, M.; Boissinot, K.; Boissinot, M.; Bissonnette, L.; Ouellette, M.; Bergeron, M. G. Microfluidic Device for Rapid (<15 min) Automated Microarray Hybridization. *Clin. Chem.* **2005**, *51*, 1836–1844.
5. Gu, H.; Xu, K.; Xu, C.; Xu, B. Biofunctional Magnetic Nanoparticles for Protein Separation and Pathogen Detection. *Chem. Commun.* **2006**, 941–949.
6. Lin, Y.-S.; Tsai, P.-J.; Weng, M.-F.; Chen, Y.-C. Affinity Capture Using Vancomycin-Bound Magnetic Nanoparticles for the MALDI-MS Analysis of Bacteria. *Anal. Chem.* **2005**, *77*, 1753–1760.
7. Gao, J. H.; Li, L. H.; Ho, P. L.; Mak, G. C.; Gu, H. W.; Xu, B. Combining Fluorescent Probes and Biofunctional Magnetic Nanoparticles for Rapid Detection of Bacteria in Human Blood. *Adv. Mater.* **2006**, *18*, 3145–3148.
8. Grossman, H. L.; Myers, W. R.; Vreeland, V. J.; Bruehl, R.; Alper, M. D.; Bertozzi, C. R.; Clarke, J. Detection of Bacteria in Suspension by Using a Superconducting Quantum Interference Device. *Proc. Nat. Acad. Sci. U.S.A.* **2004**, *101*, 129–134.
9. Kaittanis, C.; Naser, S. A.; Perez, J. M. One-Step, Nanoparticle-Mediated Bacterial Detection with Magnetic Relaxation. *Nano Lett.* **2007**, *7*, 380–383.
10. Tu, S.-I.; Uknalis, J.; Gore, M.; Irwin, P. The Capture of *Escherichia coli* O157:H7 for Light Addressable Potentiometric Sensor (LAPS) Using Two Different types of Magnetic Beads. *J. Rapid Methods Autom. Microbiol.* **2002**, *10*, 185–195.
11. Soukka, T.; Härmä, H.; Paukkunen, J.; Lövgren, T. Utilization of Kinetically Enhanced Monovalent Binding Affinity by Immunoassays Based on Multivalent Nanoparticle-Antibody Bioconjugates. *Anal. Chem.* **2001**, *73*, 2254–2260.
12. El-Boubbou, K.; Gruden, C.; Huang, X. Magnetic Glyco-nanoparticles: A Unique Tool for Rapid Pathogen Detection, Decontamination, and Strain Differentiation. *J. Am. Chem. Soc.* **2007**, *129*, 13392–13393.
13. Lin, C.-C.; Yeh, Y.-C.; Yang, C.-Y.; Chen, C.-L.; Chen, G.-F.; Chen, C.-C.; Wu, Y.-C. Selective Binding of Mannose-Encapsulated Gold Nanoparticles to Type 1 Pili in *Escherichia coli*. *J. Am. Chem. Soc.* **2002**, *124*, 3508–3509.
14. Kohler, N.; Sun, C.; Wang, J.; Zhang, M. Methotrexate-Modified Superparamagnetic Nanoparticles and Their Intracellular Uptake into Human Cancer Cells. *Langmuir* **2005**, *21*, 8858–8864.
15. Kohler, N.; Sun, C.; Fichtenholtz, A.; Gunn, J.; Fang, C.; Zhang, M. Methotrexate Immobilized Poly(ethylene glycol) Magnetic Nanoparticles for MR Imaging and Drug Delivery. *Small* **2006**, *2*, 785–792.
16. Sun, E. Y.; Josephson, L.; Kelly, K. A.; Weissleder, R. Development of Nanoparticle Libraries for Biosensing. *Bioconjugate Chem.* **2006**, *17*, 109–113.
17. Weissleder, R.; Kelly, K.; Sun, E. Y.; Shtatland, T.; Josephson, L. Cell-specific Targeting of Nanoparticles by Multivalent Attachment of Small Molecules. *Nat. Biotechnol.* **2005**, *23*, 1418–1423.

18. Hubbard, B. K.; Walsh, C. T. Vancomycin Assembly: Nature's Way. *Angew. Chem., Int. Ed.* **2003**, *42*, 730–765.
19. Walsh, C. Deconstructing Vancomycin. *Science* **1999**, *284*, 442–443.
20. Rao, J.; Colton, I. J.; Whitesides, G. M. Using Capillary Electrophoresis To Study the Electrostatic Interactions Involved in the Association of D-Ala-D-Ala with Vancomycin. *J. Am. Chem. Soc.* **1997**, *119*, 9336–9340.
21. Sundram, U. S.; Griffin, J. H. Novel Vancomycin Dimers with Activity Against Vancomycin-Resistant Enterococci. *J. Am. Chem. Soc.* **1996**, *118*, 13107–13108.
22. Kell, A. J.; Simard, B. Vancomycin Architecture Dependence on the Capture Efficiency of Antibody-Modified Microbeads by Magnetic Nanoparticles. *Chem. Commun.* **2007**, 1227–1229.
23. Lu, Y.; Yin, Y.; Mayers, B. T.; Xia, Y. Modifying the Surface Properties of Superparamagnetic Iron Oxide Nanoparticles through A Sol-Gel Approach. *Nano. Lett.* **2002**, *2*, 183–186.
24. Ma, D.; Veres, T.; Clime, L.; Normandin, F.; Guan, J.; Kingston, D.; Simard, B. Superparamagnetic Fe_xO_y@SiO_2 Core-Shell Nanostructures: Controlled Synthesis and Magnetic Characterization. *J. Phys. Chem. C.* **2007**, *111*, 1999–2007.
25. www.invitrogen.com/dynal (Accessed May 9, 2008).
26. Levine, D. P. Vancomycin: A History. *Clin. Infect. Dis.* **2006**, *42*, S5–S12.
27. Moellering, R. C. J. Vancomycin: A 50-Year Reassessment. *Clin. Infect. Dis.* **2006**, *42*, S3–S4.
28. Gu, H.; Ho, P.-L.; Tong, E.; Wang, L.; Xu, B. Presenting Vancomycin on Nanoparticles to Enhance Antimicrobial Activities. *Nano Lett.* **2003**, *3*, 1261–1263.
29. Saito, T.; Kawabata, S.; Hirata, M.; Iwanaga, S. A Novel Type of Limulus Lectin-L6. Purification, Primary Structure, and Antibacterial Activity. *J. Biol. Chem.* **1995**, *270*, 14493–14499.
30. Kannan, R.; Harris, C. M.; Harris, T. M.; Waltho, J. P.; Skelton, N. J.; Williams, D. H. Function of the Amino Sugar and N-Terminal Amino Acid of the Antibiotic Vancomycin in Its Complexation with Cell Wall Peptides. *J. Am. Chem. Soc.* **1988**, *110*, 2946–2953.
31. Lin, P.-C.; Chou, P.-H.; Chen, S.-H.; Liao, H.-K.; Wang, K.-Y.; Chen, Y.-J.; Lin, C.-C. Ethylene Glycol-Protected Magnetic Nanoparticles for a Multiplexed Immunoassay in Human Plasma. *Small* **2006**, *2*, 485–489.
32. Kell, A. J.; Somaskandan, K.; Stewart, G.; Bergeron, M. G.; Simard, B. Superparamagnetic Nanoparticle-Polystyrene Bead Conjugates as Pathogen Capture Mimics: A Parametric Study of Factors Affecting Capture Efficiency and Specificity. *Langmuir* **2008**, *24*, 3493–3502.
33. McCloskey, K. E.; Chalmers, J. J.; Zborowski, M. Magnetic Cell Separation: Characterization of Magnetophoretic Mobility. *Anal. Chem.* **2003**, *75*, 6868–6874.
34. Crowley, B. M.; Boger, D. L. Total Synthesis and Evaluation of [ψ[CH_2NH]Tpg^4]Vancomycin Aglycon: Reengineering Vancomycin for Dual D-Ala-D-Ala and D-Ala-D-Lac Binding. *J. Am. Chem. Soc.* **2006**, *128*, 2885–2892.
35. McComas, C. C.; Crowley, B. M.; Boger, D. L. Partitioning the Loss in Vancomycin Binding Affinity for D-Ala-D-Lac into Lost H-Bond and Repulsive Lone Pair Contributions. *J. Am. Chem. Soc.* **2003**, *125*, 9314–9315.